JOURNAL OF MECHANICAL ENGINEERING AND SCIENCES
ISSN: 2289-4659 e-ISSN: 2231-8380
VOLUME 17, ISSUE 3, 2023, 9629 – 9636
DOI: https://doi.org/10.15282/jmes.17.3.2023.8.0762

RESEARCH ARTICLE

Experimental and numerical investigation of the thermal and dynamic behavior of a heated vortex multijet system impacting a flat plate

A. Zerrout*, L. Loukarfi

Faculty of Technology, Department of Mechanical Engineering, University of Chlef, BP 151, 02000, Algeria
Phone: +213551194894

ABSTRACT - This study concerns the experimental and numerical study of the thermal and dynamic behavior of a configuration of a system of vortex jets impacting a flat plate, The objective of this study is to study the behavior of the thermal and dynamic field of vortex blowing of hot air from a multi-jet system impacting a flat plate. The experimental test bench comprising a support of three diffusers of diameter D, impacting the perpendicular plate. A uniform inlet temperature (T, T, T) is imposed such that the impact height H = 4D. The vortex is obtained by a vortex generator made up of 12 fins arranged at 60° from the vertical, placed just at the outlet of the diffuser. A thermo-anemometer device, to measure the blowing temperature at the point in question. The system was numerically simulated by the fluent code using a k-ε RNG turbulence model. It should be noted that the multi-jet system first appears as a free jet: going from the injection orifice to the impact zone, the axial velocity weakens, the jet undergoes considerable deflection, this is the deflection zone the velocities become mainly radial and the thickness of the boundary layer increases radially: this is the parietal flow zone, the structure of the velocity field has two zones of intense deflection with a wall jet on both sides other, favoring a good development of the resulting jet. The results show that this configuration (T, T, T) gave a better optimized distribution of temperature and velocity on the surface of the plate. This homogenization of the temperatures results from a better thermal transfer of the plate.The k-ε RNG model gave acceptable results, which coincide with those of the experimental results.

ARTICLE HISTORY
Received : 23rd Apr. 2023
Revised : 2nd Feb 2023
Accepted : 21st Aug. 2023
Published : 28th Sept. 2023

KEYWORDS
Numerical study
Thermal behaviour
Dynamic behavior
Impacting swirling jet
Flat plate
k-ε RNG model

1.0 INTRODUCTION

The impact jets find many industrial applications. Among which, there are applications comprising one or more jets such as, the drying of paper and textiles, the cooling of electronic components or turbine blades, the manufacture of glass to cool the glass sheet. In the metallurgical industry, to cool the molten metal, the cooling systems of the combustion chambers of turbojets, the cooling of turbine blades. This is internal cooling with the blade, which consists of injecting cold air through small orifices from an overpressure cavity. Icing is one of the most severe weather-related problems an aircraft can encounter. The well-known effects of icing are to increase drag, degrade aircraft control and reduce surface lift. Since the airflow around the airfoils is modified by the form of the ice, operating an aircraft in icing conditions can be very dangerous. Icing forms in the presence of supercooled water clouds or freezing rain. Ice mainly accumulates on the frontal surfaces of the aircraft: the wings, the edges of the nacelles, the windshield, the antennas, the pitot tubes and the empennage. Figure 1 shows the accumulation of ice on the wing of the airplane.

Figure 1. Icing phenomenon [1]

***CORRESPONDING AUTHOR | A. Zerrout** | ✉ zerroutamar@yahoo.fr

There are two kinds of prevention, the first is elimination on the ground: de-icing of the aircraft before departure and possible application of an effective protective liquid over a short period of time. The second method is applied in flight: anticipation / treatment of the phenomenon by switching on the anti-icing systems of certain parts of the aircraft: heating of the windscreens, propeller blades, jets of hot air impacting the edges of the attack of the aircraft wing, pitot tubes, and inflation of the leading edge tubes. Figure 2 illustrates the diagram of the anti-icing system by impacting jet, at the level of the section of an aircraft wing.

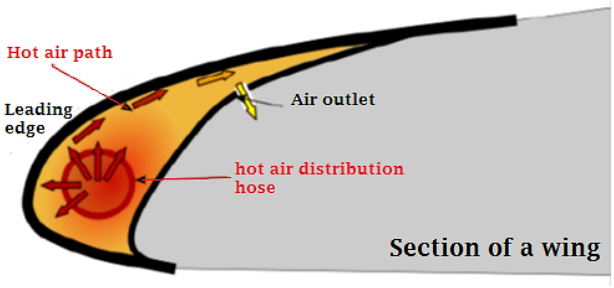

Figure 2. Anti-icing device represented at the level of the section of a wing [2]

In the structure of the impacting jet, the characteristics can be revealed according to the distance of impact and therefore according to the zone in which the impact is located. Figure 3 shows the flow of an impinging jet issuing from a nozzle in a flat plate. An impinging jet is commonly divided into three regions on the basis of the flow structure: the free jet region, the stagnation region, and the wall jet region. For high distances between the nozzle plate and the impingement plate, the free jet region has three zones:

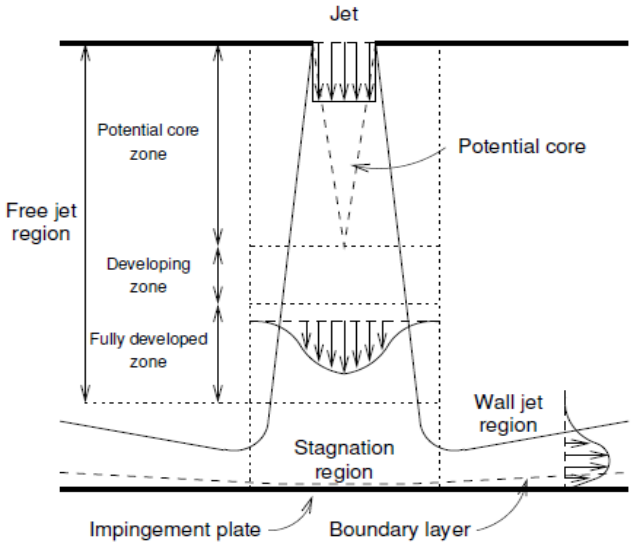

Figure 3. Flow configuration of a round impinging jet with regions of different flow regimes [3]

The following three areas: a potential core zone, a developing zone and the fully developed zone are also shown in Figure 3. In the free jet region, the shear-driven interaction of the exiting jet and the ambient produces entrainment of mass, momentum, and energy. The effects of this on the flow include the development of a non-uniform radial velocity profile within the jet, spreading of the jet, an increase of the total mass flow rate, and the modification of the jet temperature before it impinges upon the surface (only for jets with a temperature different from the ambient). In the potential core the velocity remains constant and equal to the nozzle exit velocity. Due to growth of the shear layer surrounding the potential core, the core gradually decreases in width. The length of the potential core is dependent on the turbulence intensity at the nozzle exit and the initial velocity profile [3]. Frequently reported values for the potential core length are between 4 and 6 nozzle diameters [4-6].

2.0 MATERIALS AND EXPERIMENTAL METHODS

The experimental device produced is composed of a frame (5) supporting the plate (3); the upper part is a device for blowing hot air, directed from top to bottom, comprising three diffusers (1) according to the configuration studied. This device makes it possible to scan as much as possible the space offered by a particular arrangement of the rods supporting the temperature probes (2); the temperature field is measured using an essential thermo-anemometer device (4). The probes are supported by rods that are easy to guide vertically and horizontally to scan the maximum space, a horizontal plate (3) of formica material, the temperature and velocity fields are measured at different stations in the axial and radial directions. Another thermometer used to measure the ambient T_a temperature.

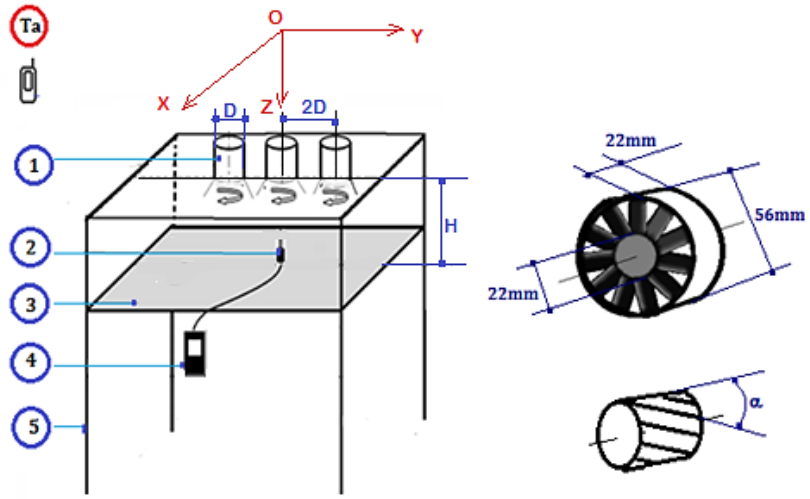

Figure 4. Experimental configuration and swirl generator [7]

2.1 The Swirl Number

The vortex is characterized by a dimensionless number that defines a measure of the ratio between the angular momentum of the axial flow and axial momentum in accordance with [8].

$$S = \frac{G_\theta}{RG_X} = \frac{\int_0^R r^2 UWdr}{R\int_0^R r\left(U^2 - \frac{W^2}{2}\right)dr} \tag{2}$$

The swirl number can be evaluated at any position of the jet because the two quantities are calculated. Swirling helps promote and improve the process of mixing and transfer, as well as the jet has the advantage of quickly flourish in free jets. Another empirical formula is used for calculating the number of swirl that the swirl number defined according to the geometric parameters of the swirl generator. This number S [9] can be written as follows:

$$S = \frac{2}{3}\left(\frac{1-\left(\frac{R_h}{R_n}\right)^3}{1-\left(\frac{R_h}{R_n}\right)^2}\right).tg\alpha \tag{2}$$

where, α is the angle of the fins built swirl generator, R_h is the radius of the vane diffuser support, R_n is the radius of diffuser. Note that in the case of a without swirler hub ($R_h = 0$), the expression becomes [10]:

$$S = \frac{2}{3}tg\alpha \tag{3}$$

In this study, the axial and tangential velocities W and U, were measured at the outlet of a diffuser with a swirling jet hot wire anemometer triple probes (DISA55M01). Four values of the swirl number can be used, S=0 to α=0°, S = 0.4 to α=30°, S=0.7 to α=45° and S=1.3 to α= 60°, respectively. According to [11], the swirl number is used, which corresponds to α=60 °.

3.0 NUMERICAL PROCEDURE

3.1 The (k-ε) (RNG) Numerical Model

A new model, based on methods using the renormalization group, has appeared in recent years. Called the k-ε RNG model, it uses a different theory from classical statistical techniques. The size of the turbulent scales is taken into account to determine which part of the energy will be transported and which will be dissipated. The small scales of turbulence which dissipate all their energy are modeled while the large scales of turbulence are studied precisely. This modeling leads to transport equations of k and ε very close to those of the standard k-ε model. The main difference comes from the constants which are no longer determined experimentally but calculated theoretically. Zhou [12] describes the evolution of k-ε RNG models.

$$\frac{\partial}{\partial t}(\rho k)+\frac{\partial}{\partial x_i}(\rho u_i k)=\frac{\partial}{\partial x_j}\left(\alpha_k \mu_{eff}\frac{\partial k}{\partial x_j}\right)+G_k+G_b-\rho\varepsilon+S_k \tag{4}$$

$$\frac{\partial}{\partial t}(\rho\varepsilon)+\frac{\partial}{\partial x_i}(\rho u_i \varepsilon)=\frac{\partial}{\partial x_j}\left(\alpha_\varepsilon \mu_{eff}\frac{\partial \varepsilon}{\partial x_j}\right)+C_{1\varepsilon}\frac{\varepsilon}{k}(G_k+G_{3\varepsilon}G_b)-C_{2\varepsilon}\rho\frac{\varepsilon^2}{k}+S_\varepsilon \tag{5}$$

where, $C_\mu = 0.0845$, $C_{\varepsilon 1} = 1.42$ $C_{\varepsilon 2} = 1.68$, $C_{\varepsilon 2} = 1.68$, $\alpha_\varepsilon = 1.393$ and μ_{eff} is the effective viscosity.

3.2 Numerical Method and Computational Domain

The computational domain is divided into a number of volumes called superposed control volume such that each volume surrounding each point of the mesh. Calculations have been tested on different meshes for the control of the solution, in order to seek the limit of the independence of the solution in relation to the fineness of the mesh, especially in the regions close to the blowing orifices of the diffuser, while respecting the basic rules that make an acceptable grid. It can be seen that the solution of the requested variables does not change significantly. Calculations are limited to a number of 226284 nodes. in conclusion that the affinity of the mesh is acceptable and the solution is independent of the mesh. As the geometry is regular, the generation of the mesh was carried out using the mesher, with tetrahedral meshes with four nodes.

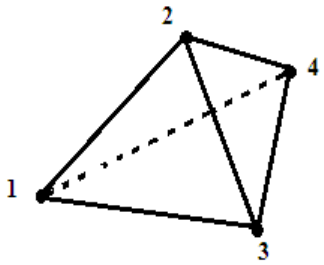

Figure 5. Tetrahedral mesh with 4 nodes

The differential equation is integrated for each volume control and the result of this integration gives the discrete equation expressed using the values of the function φ (scalar quantity) for a set of grid points according to:

$$\underbrace{\frac{\partial(\rho.r.U_i.\varphi)}{\partial X}}_{Convection}=\underbrace{\frac{\partial}{\partial X}\left(r.\Gamma.\frac{\partial\varphi}{\partial X}\right)+\frac{\partial}{\partial X}\left(r.\Gamma.\frac{\partial\varphi}{\partial r}\right)}_{Diffusion}+\underbrace{r.S_\varphi}_{source} \tag{6}$$

where, φ can be assimilated to any transportable physical quantity (U, V, W, k, ε and others), Γ is thediffusion coefficient which depends on the particular significance of the variable to be processed. The discrete equation obtained expresses the principle of conservation for φ on the volume control in the same manner that the differential equation expressed for an infinitesimal volume control by applying the theory exposed by [13].

3.3 Conditions to the Limits

The boundary conditions are necessary at the start of the calculation program and can have a significant effect on the numerical results. The operating constraints can be resumed in the following field of study with the following diagram in Figure 6. Here, the velocity inlet, U=10 m/s, inlet temperature, T=363 °K, pressure outlet, P=P_{atm} and Ta=300 °K.

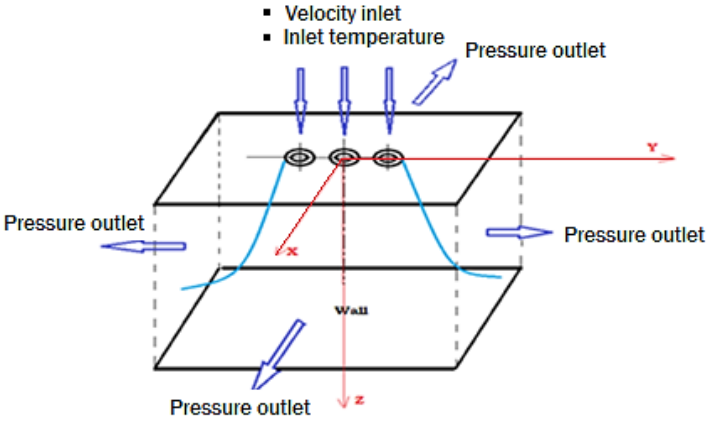

Figure 6. The boundary conditions of the domain of the studied configuration

4.0 RESULTS AND DISCUSSION

4.1 Reduced Numerical Temperature Profiles

Figure 7 shows the superimpositions of the profiles of the reduced temperature T_r in the plane (y, z), with an impact height H = 4D, for an inlet configuration at the diffuser (T, T, T). These profiles ensure symmetry with respect to the axis of the central jet. The gaits present maximums at the output levels of the diffusers in the first stations (Z = 0.5D, 1D, 2D). Temperature drops when moving downstream of the jet and in the mixing zone of the jet. In the following stations, the temperature amplitudes decrease significantly from one station to another to reach the impact temperature at the level of the jet deflection zone. This configuration presents a good temperature homogenization on the wall of the plate.

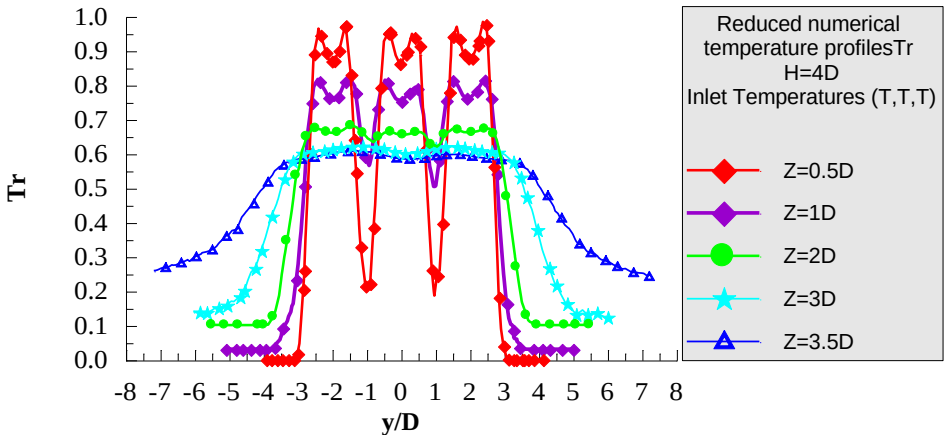

Figure 7. Reduced numerical temperature T_r profiles with, inlet temperatures (T, T, T), impact height H = 4D, station Z = 3.5D

4.2 Reduced Numerical Velocity Profiles

Figure 8 shows the superposition of the profiles of the reduced velocity U_r as a function of the radial distance y/D, with a uniform distribution of the blowing velocities at the inlet of the diffuser (U,U,U). By examining this figure, it is noted that the curves of the reduced velocity present maximum amplitudes at the level of the potential core of each jet (near the blowing orifice). These amplitudes become lower and lower as they move away from the impact region. The dimensionless average velocity U_r decreases as one moves downstream and becomes nearly parallel to the plate. Thus, the mixture exhibits a low overall jet spread.

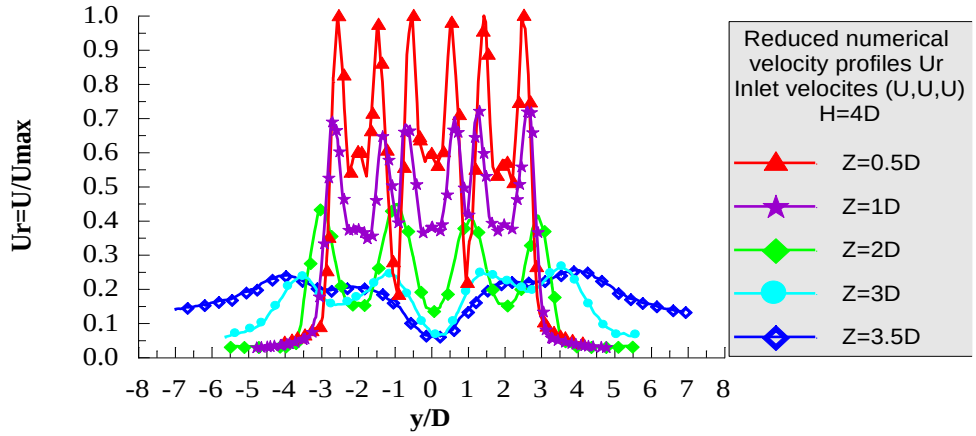

Figure 8. Reduced numerical velocity profiles U_r with inlet velocities (U, U, U), impact height H = 4D, station Z = 3.5D

4.3 Temperature Field

The Figure 9 exposes the temperature field of the mixture resulting from the multi-jet system impacting a plate for an impact height H = 4D, with the configuration of inlet temperatures at the diffusers (T,T,T). This configuration having a balanced temperature distribution and a balanced flow at the inlet of the diffuser with swirling, ensures a uniform and homogeneous temperature distribution along the plate, and producing heat transfer over the entire heat exchange surface of the plate.

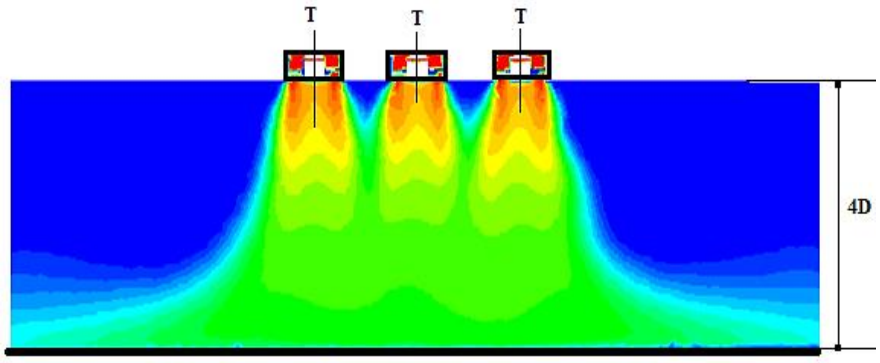

Figure 9. Temperature field

The Figure 10 exposes the temperature field lines of the multijet system impacting the plate. The field being symmetrical with respect to the main axis of the jet, a complete and balanced spread of heat transfer over the entire surface. By examining the temperature lines in the impact zone, it can be said that the temperature reaches the entire surface of the plate, which favors a homogeneity of the heat transfer over the entire wall of the plate.

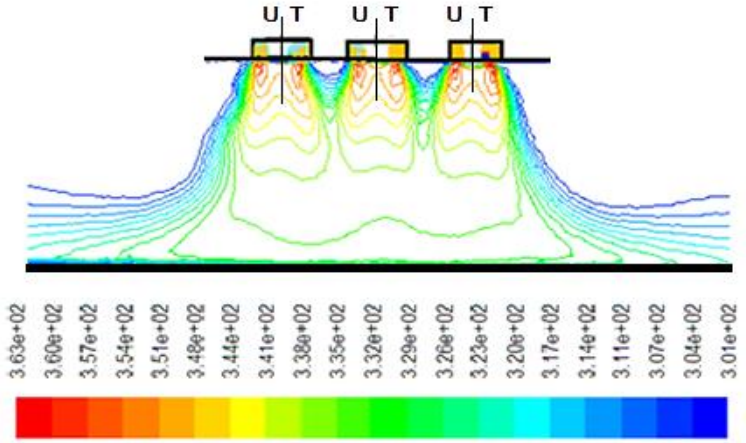

Figure 10. Contour temperature field

4.4 Velocity Vector Field

In the Figure 11, the velocity field has been represented (for an impact height H = 4D, with inlet velocities at the balanced diffusers (U,U,U). Note that the multi-jet system first appears as a free jet from the injection orifice to the end of the potential cone: this is the established flow zone, then its axial velocity weakens, then the jet deviates from its initial axial direction: this is the deflection zone where the velocities become mostly radial and the thickness of the boundary layer increases radially: this is the parietal flow zone. In this configuration, having a uniform velocity distribution at the level of the diffusers, the structure of the velocity field presents two zones of intense and symmetrical deflection with respect to the axis of the jet, with a wall jet on either side, favoring a good development of the resulting flow.

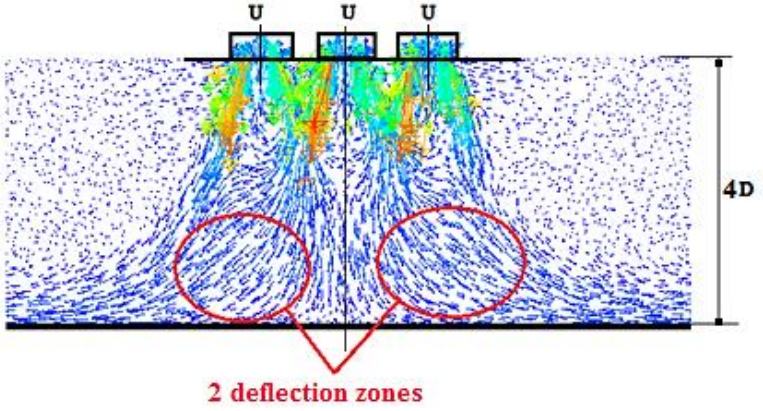

Figure 11. Velocity vector fields

4.5 Validation of Results

The quality of comparison between the numerical results and experimental results comparison is evidenced in Figure 12 and Figure13 in terms of reduced temperature T_r. The numerical results of the model with two transport equations k-ε RNG used to simulate this case are in good agreement with experimental results. However, there is a difference, which is not important between the numerical appearance and the experimental points in the first stations; this is due to measurement uncertainties. The model k-ε RNG considers an isotropic turbulent viscosity without omitting the influence of uncertainties of measurements operated on. Despite the shortcomings, the model k-ε RNG gave acceptable results qualitatively. Nevertheless, it is a relatively simple and inexpensive simulation tool.

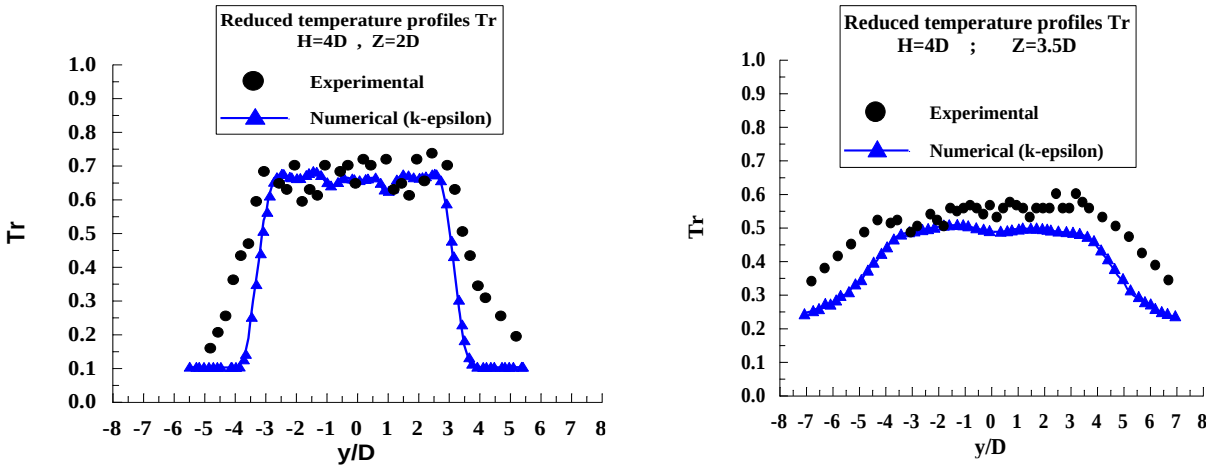

Figure 12. Comparison of the numerical temperature profiles T_r with the experimental points in the plane (Y, Z) for the configuration (T,T,T), station 2D and 3.5D with impact height h = 4D

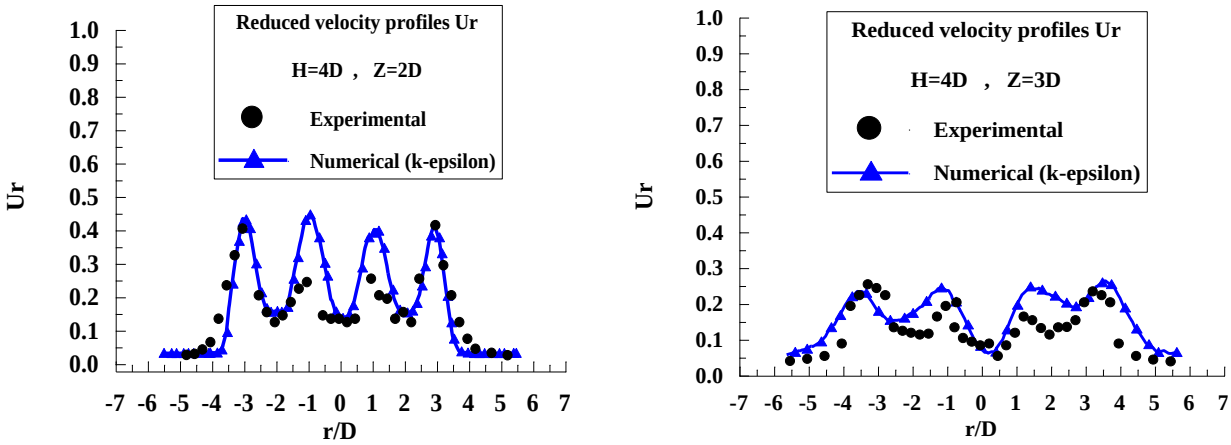

Figure 13. Comparison of the numerical velocity profiles U_r with the experimental points in the plane (Y, Z) for the configuration (U,U,U), station 2D and 3.5D with impact height h = 4D

5.0 CONCLUSIONS

The present study clearly shows that, at the beginning, the jet has the same characteristics as a free jet. Very close to the obstacle, it undergoes a considerable deflection characterized by the weakening of the velocities and the expansion of the jet (the amplitudes of temperature decrease). On contact with the plate, the curves become almost parallel to the plate, and the velocities change direction and develop radially. The swirling ensures thermal homogenization with a large spread. The presence of the plate reduces the temperature amplitudes as well as the recirculation zone, the temperature of the plate decreases as it moves away from the diffuser and becomes negligible beyond ten diameters of the blowing orifice. Furthermore, the optimum configuration of a multiple impact plate jet system that provides optimum temperature on the plate wall depends on the inlet temperature distribution of the diffusers and the airflow rates at the inlet of the diffusers. By examining the structure of the temperature field after diffusion of the jets, the temperature contours reach the entire surface of the plate favoring a homogenization of the heat transfer of the plate. This configuration of swirling multi-jets allows a perfect distribution of the jets with a homogenization of the heat transferring the plate. This mixing ratio can be influenced by other parameters, such as the direction of the vortex of the central jet, the inclination of the axes of the lateral jets, the variation of the center distance, the geometry of the diffusers and others. The comparison between the numerical results and the experimental results presented in this study indicates that the k-ε RNG model

produces satisfactory and comparatively acceptable results. The latter remains a relatively simple and inexpensive simulation tool to use.

6.0 ACKNOWLEDGMENTS

This research was supported by the laboratory of test, measurement, and mechanical simulation of the University of Chlef. The author expresses his gratitude to the Department of Mechanics of the Faculty of Technology, Hassiba Benbouali University of Chlef, Algerian Republic for their support during the experimental study of the impacting multi-jet system within the laboratory.

7.0 REFERENCES

[1] T. Turner, "Aviation Safety: Top three aircraft icing myths busted," Available*:* https://www.aviationsafetymagazine.com/. Accessed: April 2023.

[2] M. Francois and Y. Saleh, "Impinging spray technique for ground deising," *Aeronautics and Aerospace Research Article*, pp. 1 - 6, 2016.

[3] R. Viskanta, "Heat transfer to impinging isothermal gas and flame jets," *Experimental Thermal and Fluid Sciences*, vol. 6, no. 2, pp. 111-134, 1993.

[4] J. N. B. Livingood and P. Hrycak, "Impingement heat transfer from turbulent air jets to flat plates – A literature survey," *National Aeronautics and Space Administration*, Technical report NASA TM X-2778, pp. 1 - 42, 1973.

[5] K. Kataoka, "Impingement heat transfer augmentation due to large scale eddies," in *Proceeding of 9th International Heat Transfer Conference*, pp. 255–273, 1990.

[6] D. Cooper, D. C. Jackson, B. E. Launder and G. X. Liao, "Impinging jet studies for turbulence model assessment - I. Flow-field experiments," *International Journal of Heat and Mass Transfer*, vol. 36, no. 10, pp. 2675–2684, 1993.

[7] A. Zerrout, "Experimental and numerical study of impacting swirling multi-jet system," *Doctoral Thesis*, University of Chlef, Algeria, 2016.

[8] A. K. Gupta, D. G. Lilley, N. Syred, "Swirl flows*," Abacus Press*, Tunbridge Wells, England, 1984.

[9] Y. Huang, and V. Yang, "Dynamics and stability of lean-premixed swirl-stabilized combustion," *Progress in Energy and Combustion Science*, vol. 35, no. 4, pp. 293-364, 2009.

[10] H. Sato, M. Mori, and T. Nakamura, "Development of a dry ultra-low NOx double swirler staged gas turbine combustor", *Journal of Engineering for Gas Turbine and Power*, vol. 120, no. 1, pp. 41-47, 1998.

[11] M. Braikia, L. Loukarfi, A. Khelil, and H. Naji, "Improvement of thermal homogenization using multiple swirling jets," *Thermal Science*, vol. 16, no. 1, pp. 239-250, 2021.

[12] X. Zhou, Z. Sun, G. Bernner, and F. Durst, "Combustion modelling of turbulent jet diffusion, H_2/air flame with detailed chemistry," *International Journal of Heat and Mass Transfer*, vol. 43, pp. 2075-2088, 2000.

[13] S. V. Patankar, "Numerical heat transfer and fluid flow," *Hemisphere Publishing Corporation*, USA, 1980.